Front. Optoelectron. China 2011, 4(1): 121–127
DOI 10.1007/s12200-011-0165-6

RESEARCH ARTICLE

Photochemical synthesis and photocatalysis application of ZnS/amorphous carbon nanotubes composites

Zhen FANG (✉), Yueting FAN, Yufeng LIU

Anhui Key Laboratory of Functional Molecular Solids, College of Chemistry and Materials Science, Anhui Normal University, Wuhu 241000, China

Abstract In this paper, a photochemical synthesis of ZnS-amorphous carbon nanotubes (ACNTs/ZnS) composites using ACNTs was reported, whose surface were modified with carboxylic groups as a support. The size and distribution of ZnS nanoparticles can be controlled by adjusting the initial amount of reactants and the reaction time. The ACNTs/ZnS nanocomposites were characterized by X-ray power diffraction, scanning electron microscopy and transmission electron microscopy. Studies showed that ACNTs/ZnS nanocomposites had high photocatalytic activity toward the photodegradation of dye molecule.

Keywords nanocomposite, photochemical synthesis, photodegradation

1 Introduction

As an important II-VI semiconductor with wide band gap, ZnS has been attracting extensive attention and has been applied in photocatalysis, optoelectronic devices, and sensors due to its unique optical and electrical properties [1–3]. Various methods had been used to synthesize nanostructural ZnS. For example, ZnS nanoporous nanoparticles were prepared by solution-phase thermal decomposition route using zinc acetate and thiourea as Zn and S sources, respectively [4]. ZnS nanotubes were self-assembled via a thermochemistry process using ZnS powers as precursors [5]. Owing to the fast generation of electron-hole pairs in photocatalysis reaction, ZnS nanocrystals have been used as photocatalyst in photodegadation of organic pollutions [4]. However, a problem is that the ZnS nanocrystals incline to agglomerate in solution and then affect the photocatalysis effection. Therefore, TiO_2, CuS and carbon nanotubes had been used as a support to enhance the photocatalytic activity [6–8]. Recently, we have prepared carboxyl modified amorphous carbon nanotubes (ACNTs) by a simple solvothermal method. Thanks to its large surface area, ACNTs were a good candidate for the support to keep the nanoparticles from agglomeration.

Due to the efficient energy of photons provided by the light, the photochemical route is a convenient, mild and environmental friendly method for synthesis of metal and sulfide nanomaterials [9–11]. However, the previous work using photochemical method were focused on preparing nanoparticles, while the synthesis of nanocomposite through photochemical reaction is scarcely reported [12]. Herein, we use carboxyl modified ACNTs as a support and the ultra-violet (UV) lamp as light source to synthesize ACNTs/ZnS nanocomposites. The as-synthesized ACNTs/ZnS nanocomposites exhibit excellent photocatalytic activity to dye molecule under UV light.

2 Materials and method

2.1 Materials

Ferrocenecarboxylic acid, carbon disulfide (CS_2), toluene, carbon tetrachloride, $Zn(Ac)_2 \cdot 2H_2O$, thioacetamide (TAA), eosin, methyl blue (MB) and methyl red (MR) are all analytic-grade chemical reagents (Shanghai Chemical Co.) and used without purification.

2.2 Synthesis of ACNTs

In a typical procedure, 0.23 g ferrocenecarboxylic acid was dissolved in 34 mL of toluene, and then, 0.2 mL of carbon tetrachloride and 6 mL of carbon disulfide (CS_2) were added into the above solution. The solution was sealed in a Teflon-lined stainless steel autoclave and maintained at

Received October 18, 2010; accepted December 30, 2010

E-mail: fzfscn@mail.ahnu.edu.cn

200°C for 12 h. The sponge-like black products were collected and washed with alcohol and distilled water.

2.3 Synthesis of ACNTs/ZnS nanocomposites via photochemical reaction

In the Synthesis of ACNTs/ZnS nanocomposites, 2 mg of ACNTs was dispersed in 15 mL of distilled water with strong ultrasonic. Then, 0.2 mmol of $Zn(Ac)_2 \cdot 2H_2O$ and 0.2 mmol of TAA were added to the above solution to form a homogeneous solution by continuous stirring. To obtain the ACNTs/ZnS nanocomposites, we exposed the mixed solution under a 300 W high-pressure mercury lamp (wavelength centered at 365 nm) for 1 h. Magnetic stirring was applied throughout the entire synthesis. The products (named sample D) were filtrated and washed by alcohol and distilled water.

We found that the size and distribution of ZnS nanoparticles which were deposited on ACNTs changed with different experimental parameters. To study the effect of experimental parameters, we experience a series of contrastive experiments by altering the initial amount reactants and reaction time. In the above contrastive experiments, the amounts of ACNTs were kept as 2 mg. The detailed experimental parameters are listed in Table 1.

2.4 Photocatalytic testing

The photocatalytic activity of the ACNTs/ZnS nanocomposites was evaluated by degrading eosin, MB and MR aqueous solution (50 mL) with 10 mg as-prepared ACNTs/ZnS nanocomposites under UV irradiation at ambient temperature. Experimental details were as follows: 10 mg of the ACNTs/ZnS nanocomposites was dispersed in a 50 mL of the dye solution (0.01 g/L) in a 100 mL beaker. The solution was stirred in dark for 6 h and then irradiated for 80 min with a 300 W UV lamp (Yaming Lighting Co., Ltd., 10 cm above the solution) with wavelengths centered at 365 nm. 5 mL solution was taken out of the system at 10 min time interval and centrifuged at 9000 r/min for 3 min. The concentration of the dye was determined with a Shimadzu U-3010 UV-vis spectrophotometer.

2.5 Characterization

The X-ray powder diffraction patterns were obtained by a Shimadzu X-ray diffractometer (XRD, Shimadzu, XRD-6000). Scanning electron microscopy (SEM, Hitachi, S-4800), high resolution transmission electron microscopy (HRTEM, JEOL-2010) and UV-vis absorption spectroscopy (Shimadzu, U-3010) were used to measure the morphology, structure, size and optical response of the product. The Raman spectrum was recorded at ambient temperature on a LABRAM-HR confocal laser micro-raman spectrometer with an argon-ion laser at an excitation wavelength of 514.5 nm. The infrared spectrum was collected on a Shimadzu IR prestige-21 Fourier transform-infrared (FT-IR) spectrum in the wavelength range from 400 cm^{-1} to 4000 cm^{-1}. Photoluminescence (PL) spectrum of the as-obtained samples was measured on an Edinburgh 920 fluorescence spectrophotometer using a 325 nm excitation line at room temperature.

3 Results and discussion

SEM and TEM were used to determine the morphology and microstructure of the ACNTs. Figure 1(a) is the SEM image of the as-prepared ACNTs. It reveals that we obtained a large quantity of ACNTs with uniform size. The TEM image of ACNTs, the dark wall and light inner of products, is shown in Fig. 1(b), giving the direct evidence of tubular structure. From the TEM image, we observed that the diameter of carbon nanotubes was about 100 nm and the wall thickness was about 25 nm. It should be noted that as-obtained carbon nanotubes had smooth surface. HRTEM images of a small area of nanotube were shown in Fig. 1(c), indicating that the CNTs were amorphous.

Figure 2(a) shows the XRD pattern of the ACNTs, only a broad and weak peak at around 20°, indicating that the as-prepared carbon nanotubes is amorphous. Two peaks are observed in Raman patterns. One peak is observed at around 1586 cm^{-1} named G-band, which is related to the vibration of sp^2-bonded carbon atoms in the hexagonal graphitic plane. The other peak is at 1370 cm^{-1} named D-band, which corresponds to the vibrations of carbon atoms with dangling bonds in disorder graphite planes [13,14]. Figure 2(c) shows the IR patterns of the ACNTs. The weak peak at 1606 cm^{-1} is the C = O stretching vibrations of carbonyl groups; the peak at around 1702 cm^{-1} is assigned to the – COOH stretch; the peak at around 2941 cm^{-1} is the O-H stretching vibration of carbonyl groups [15]. The peak at 2350 cm^{-1} indicates that CO_2 is adsorbed on the surface of ACNTs. The present results indicate that as-obtained ACNTs were modified with carboxylic groups during preparation without further treating.

Table 1 Summary of experimental parameters

sample	A	B	C	D	E	F
$Zn(Ac)_2 \cdot 2H_2O$/mmol	0.8	0.6	0.4	0.2	0.2	0.2
TAA/mmol	0.8	0.6	0.4	0.2	0.2	0.2
reaction time	1 h	1 h	1 h	1 h	30 min	10 min

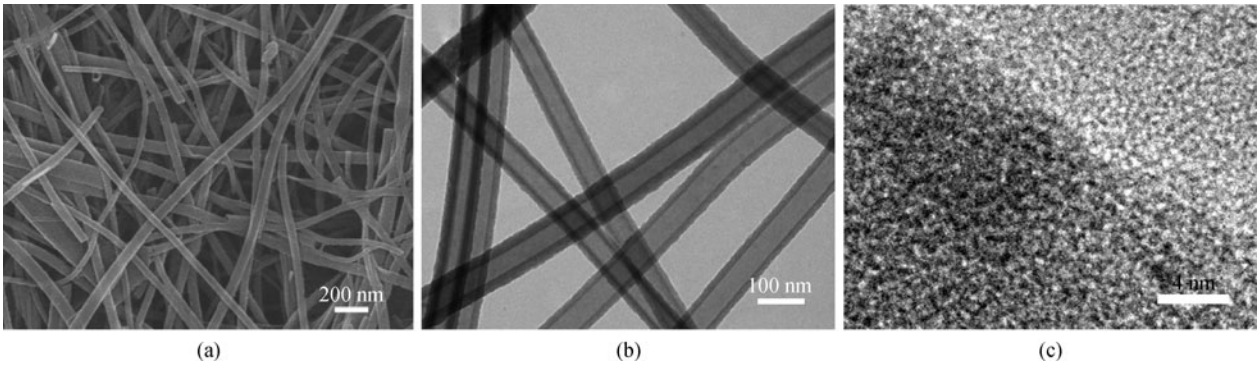

Fig. 1 Images of ACNTs. (a) SEM; (b) TEM; (c) HRTEM

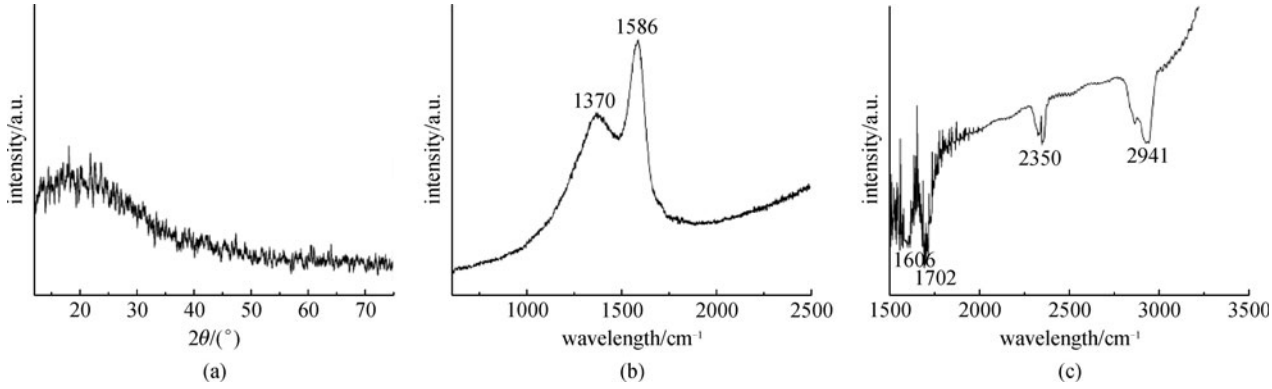

Fig. 2 Patterns of ACNTs. (a) XRD; (b) Raman; (c) IR

Figure 3(a) is the XRD pattern of ACNTs/ZnS nanocomposites. Three apparent peaks correspond respectively to the crystal planes of the (111), (220), and (311) of face-centered cubic ZnS, consistenting with the standard diffraction date (JCPDS Card File No. 80-0020). The peaks are broad, indicating that the size of ZnS nanoparticles is small. The SEM image of ACNTs/ZnS nanocomposites is shown in Fig. 3(b), in which the roughness surface of the products reveals that ZnS nanoparticles are deposited on ACNTs successfully. From the high-magnification TEM image of ACNTs/ZnS nanocomposites (sample D) in Fig. 3(c), we observed that ZnS nanoparticles were well dispersed on ACNTs with uniform sharp along the axis of ACNTs. The size of ZnS nanoparticles is about 50 nm. The HRTEM image (Fig. 3(d)) of ZnS nanoparticles shows that the lattice fringes on the crystal face have a spacing of 0.3 nm, corresponding to the (111) plane of cubic ZnS. A selected area electron diffraction pattern of ZnS nanoparticles is presented in the inset of Fig. 3(d). The concentric rings of electron diffraction pattern indicate that the ZnS nanoparticles are polycrystalline.

We investigated the influence of initial amount of $Zn(Ac)_2 \cdot 2H_2O$ and TAA by varying the initial amount as 0.8, 0.6, and 0.4 mmol. The corresponding images are shown in Figs. 4(a)–(c). When the initial amount of Zn $(Ac)_2 \cdot 2H_2O$ was decreased from 0.8 mmol to 0.4 mmol, the size of ZnS nanoparticles was decreased from 500 to 100 nm. Meanwhile, the percentage of coverage and the quantity of ACNTs/ZnS nanocomposites were improved. When 0.8 mmol $Zn(Ac)_2 \cdot 2H_2O$ was used, only few ZnS nanoparticles are aggregated and deposited on ACNTs with large size (500 nm, Fig. 4(a)), and a large number of ZnS nanoparticles exist in the products. It indicates that the excess ZnS may not favor the homogenous growth of ACNTs/ZnS nanocomposites. When only 0.4 mmol of $Zn(Ac)_2 \cdot 2H_2O$ was added, the deposited ZnS nanoparticles are uniform with sizes about 100 nm (Fig. 4(c)). One reasonable explanation is that, along with the decrease of Zn and S source, the amount of ZnS nuclei decreases, leading to the decrease of the size of ZnS nanoparticles. The results show that the amounts of reactant play an important role in the synthesis of ACNTs/ZnS nanocomposites. It has to be noted that ACNTs became shorter after the deposit of ZnS nanoparticles. The phenomenon can be explained as follows. A large quantity of ZnS nanoparticles were deposited on ACNTs through chemical bond, leading to the reduction of the carbon-carbon bond energy of ACNTs. Thus, UV irradiation may provide enough energy to cutting off the ACNTs.

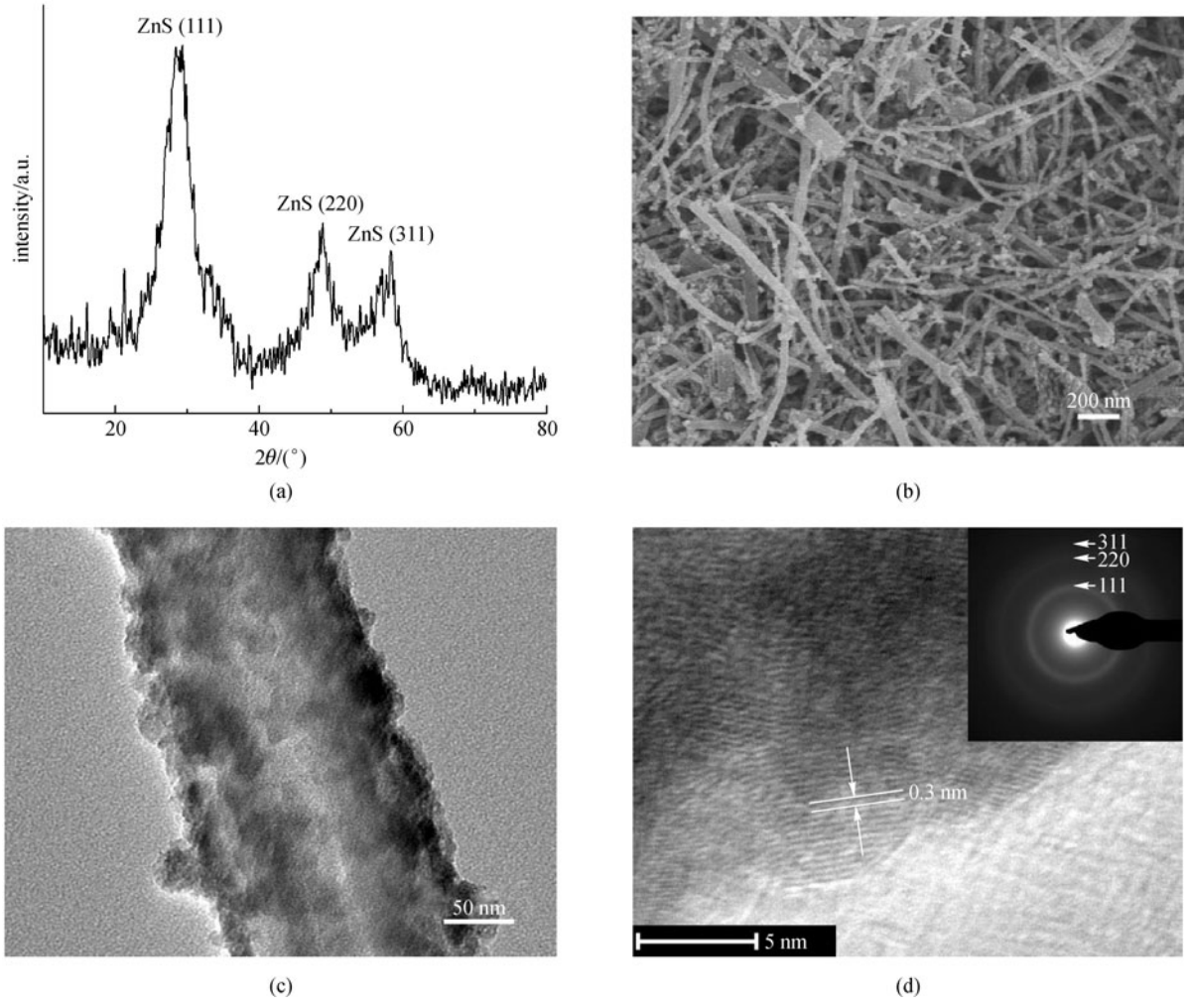

Fig. 3 Images of ACNTs/ZnS nanocomposites. (a) XRD; (b) SEM; (c) TEM; (d) HRTEM (insert is electron diffraction pattern)

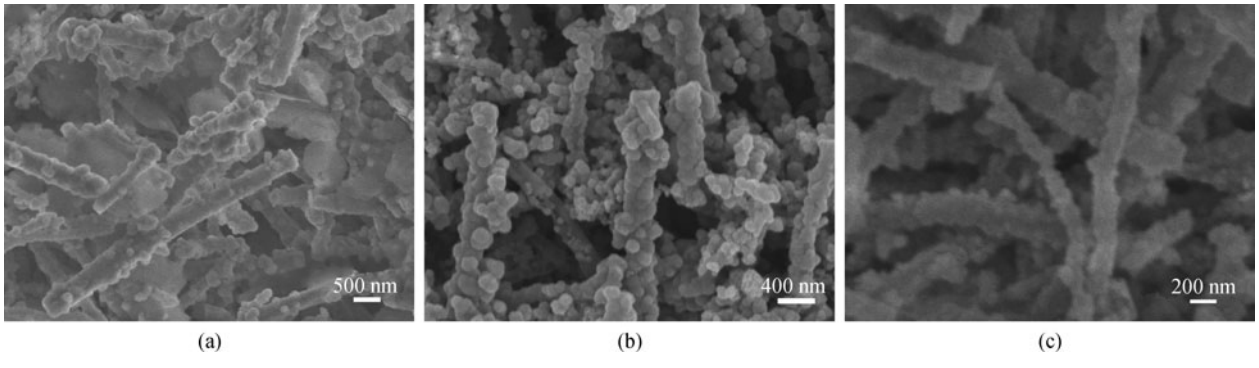

Fig. 4 SEM images of ACNTs/ZnS nanocomposites corresponding to samples A –C in Table 1. (a) A; (b) B; (c) C

The effect of reaction time was also investigated, the corresponding images were shown in Fig. 5. When the reaction time was increased from 10 min to 1 h, the size of ZnS nanoparticles is increased from 20 nm to 50 nm. When the system only reacted for 10 min, only few ZnS nanoparticles are deposited on ACNTs with the size of around 20 nm (Fig. 5(a)). Along with the reaction proceeding, the size and coverage of ZnS nanoparticles are increased and at last the uniform ZnS nanoparticles are deposited on ACNTs surface. On the basis of our

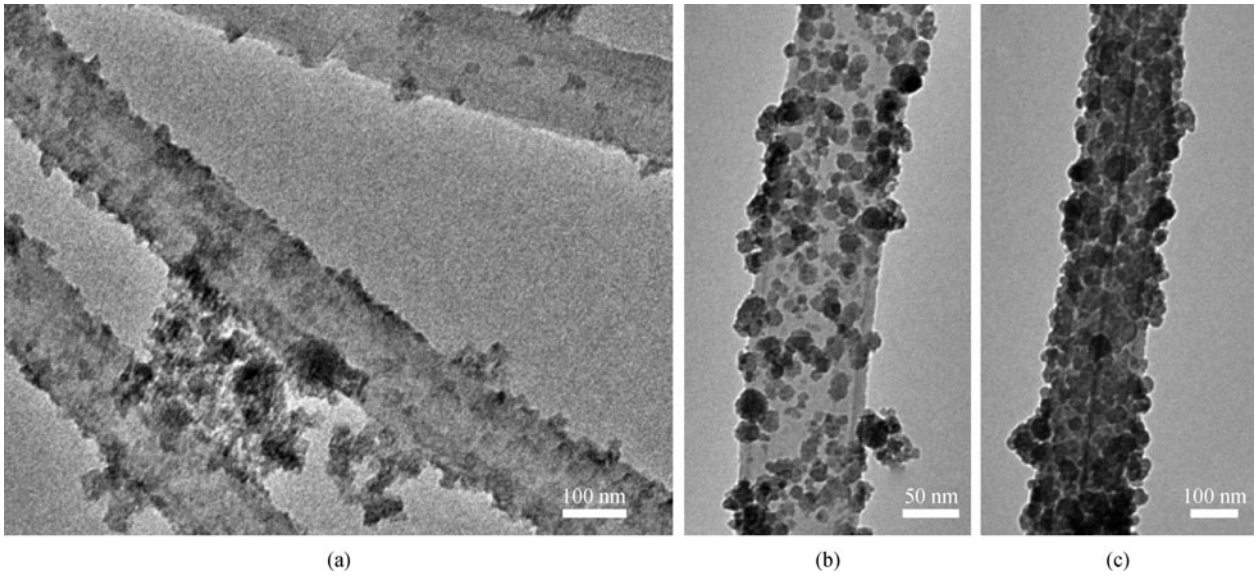

Fig. 5 TEM images of ACNTs/ZnS nanocomposites prepared with different reaction time. (a)10 min; (b) 30 min; (c) 1 h

experiment process of synthesizing ACNTs/ZnS nanocomposites, a probable formation mechanism is proposed. Amorphous carbon nanotubes were used as substrate for deposition ZnS nanoparticles. At first, the positive metal ions Zn^{2+} were adsorbed onto the surfaces of ACNTs by electrostatic attraction. And then, S^{2-} ions were released from TAA due to the UV irradiation. The S^{2-} ions will be heterogeneously nucleated with Zn^{2+} ions to form ZnS nanoparticles on the surfaces of ACNTs. UV irradiation improved the decomposition of TAA and nucleation rate of ZnS nanoparticles. The main formation mechanism is depicted in Fig. 6.

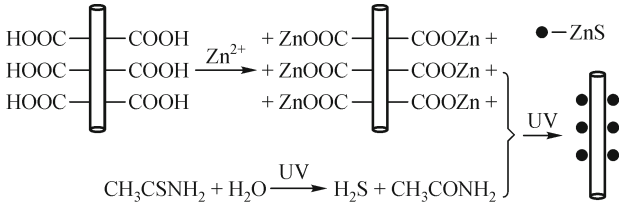

Fig. 6 Formation mechanism of ACNTs/ZnS nanocomposites

The photoluminescence spectrum of ZnS materials was complicated, with different structures having different spectra. Figure 7 depicts the photoluminescence spectrum of ACNTs/ZnS nanocomposites (sample D) and two emission bands are observed in the spectrum. One band at around 430 nm, which is attributed to the surface defect states. The other band is at around 474 nm, which is related to the self-activated defect centers [16].

As the ZnS nanoparticles are homogenously deposited on ACNTs with small size, the ACNTs/ZnS nanocomposites may have an improved photocatalytic activity. The

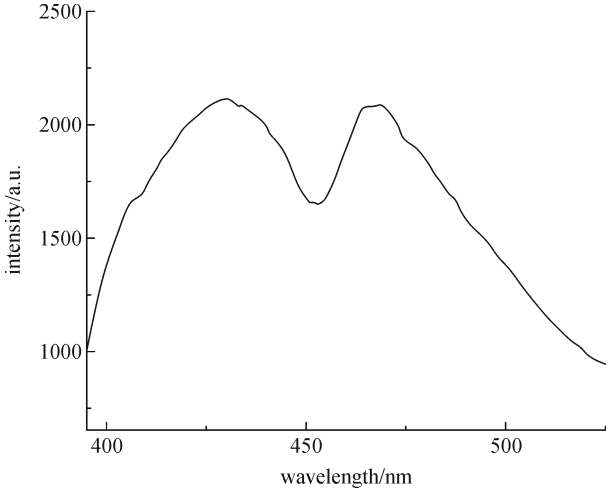

Fig. 7 Photoluminescence spectrum of ACNTs/ZnS nanocomposites

photocatalytic activity of the as-prepared ACNTs/ZnS nanocomposites (sample D) was evaluated by monitoring the absorption spectrum of MB, eosin and MR. In the case of MB and eosin, the dye was decolorized completely after about 50 min (Figs. 8(a) and 8(b)). As for MR, it needs 80 min for the entire degradation (Fig. 8(c)). Our results show that the as-prepared ACNTs/ZnS nanocomposites exhibit an efficient photocatalytic activity for different organic dye molecule, although the efficiency of the nanocomposites is different (Fig. 8(d)). The efficient degradation of the dye should be ascribed to that ZnS nanoparticles deposited on the surfaces of ACNTs had elevated specific surface area. Under the irradiation of UV, electrons and holes are generated in ZnS nanoparticles,

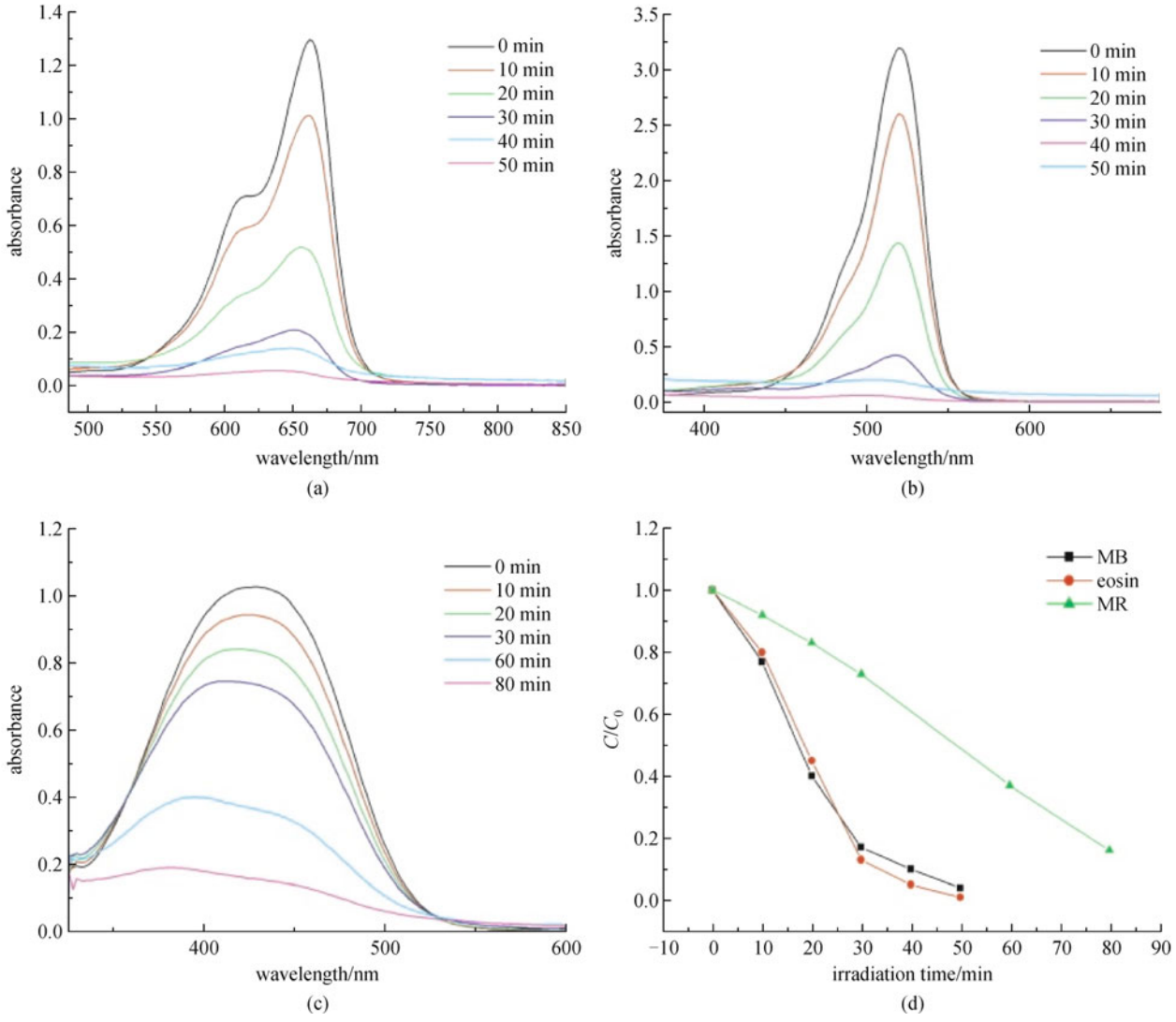

Fig. 8 Absorption spectra of different dyes degraded by ACNTs/ZnS nanocomposites. (a) MB; (b) eosin; (c) MR; (d) photodegradation rate of different dyes

meanwhile, the elevated specific surface area affords more active sites for photochemical reaction and thus enhance the photocatalytic activity.

4 Conclusions

An efficient photochemical route to synthesize ACNTs/ZnS nanocomposites has been proposed. For the abundant carboxyl groups on the ACNTs surface, ZnS nanoparticles can be easily deposited on it. The as-prepared ACNTs/ZnS nanocomposites contain ACNTs with a diameter about 100 nm and ZnS nanoparticles with sizes ranging from 50–500 nm. Photocatalysis study indicates the ACNTs/ZnS nanocomposites exhibit good activity for photodegradation of the organic dye molecule. The nanocomposites synthesized by this photochemical route are expected to find more applications in catalysts and photoelectricity fields.

Acknowledgements This work was supported by the National Natural Science Foundation of China (Grant No. 20701002).

References

1. Yin L W, Bando Y, Zhan J H, Li M S, Golberg D. Self-assembled highly faceted wurtzite-type ZnS single crystalline nanotubes with hexagonal cross-section. Advanced Materials (Deerfield Beach, Fla.), 2005, 17(16): 1972–1977
2. Moore D F, Ding Y, Wang Z L. Crystal orientation-ordered ZnS nanowire bundles. Journal of the American Chemical Society, 2004, 126(44): 14372–14373
3. Shen G Z, Bando Y, Golberg D. Self-assembled three-dimensional

structures of single-crystalline ZnS submicrotubes formed by coalescence of ZnS nanowires. Applied Physics Letters, 2006, 88 (12): 123107

4. Hu J S, Ren L L, Guo Y G, Liang H P, Cao A M, Wan L J, Bai C L. Mass production and high photocatalytic activity of ZnS nanoporous nanoparticles. Angewandte Chemie International Edition, 2005, 44(8): 1269–1273
5. Fang X S, Ye C H, Zhang L D, Wang Y H, Wu Y C. Temperature-controlled catalytic growth of ZnS nanostructures by the evaporation of ZnS nanopowders. Advanced Functional Materials, 2005, 15 (1): 63–68
6. Zhang Z H, Yuan Y, Fang Y J, Liang L H, Ding H C, Jin L T. Preparation of photocatalytic nano-ZnO/TiO_2 film and application for determination of chemical oxygen demand. Talanta, 2007, 73(3): 523–528
7. Yu J G, Zhang J, Liu S W. Ion-exchange synthesis and enhanced visible-light photoactivity of CuS/ZnS nanocomposite hollow spheres. Journal of Physical Chemistry C, 2010, 114(32): 13642–13649
8. Wu H Q, Wang Q Y, Yao Y Z, Qian C, Zhang X J, Wei X W. Microwave-assisted synthesis and photocatalytic properties of carbon nanotube/zinc sulfide heterostructures. Journal of Physical Chemistry C, 2008, 112(43): 16779–16783
9. Kundu S, Wang K, Liang H. Photochemical generation of catalytically active shape selective rhodium nanocubes. Journal of Physical Chemistry C, 2009, 113(43): 18570–18577
10. Zhao W B, Zhu J J, Xu J Z, Chen H Y. Photochemical synthesis of Bi_2S_3 nanoflowers on an alumina template. Inorganic Chemistry Communications, 2004, 7(5): 847–850
11. Jana S, Pande S, Sinha A K, Sarkar S, Pradhan M, Basu M, Saha S, Pal T. A green chemistry approach for the synthesis of flower-like Ag-doped MnO_2 nanostructures probed by surface-enhanced raman spectroscopy. Journal of Physical Chemistry C, 2009, 113(4): 1386–1392
12. Chen S F, Li J P, Qian K, Xu W P, Lu Y, Huang W X, Yu S H. Large scale photochemical synthesis of M@TiO_2 nanocomposites (M = Ag, Pd, Au, Pt) and their optical properties, CO oxidation performance, and antibacterial effect. Nano Research, 2010, 3(4): 244–255
13. Shao M W, Wang D B, Yu G H, Hu B, Yu W C, Qian Y T. The synthesis of carbon nanotubes at low temperature via carbon suboxide disproportionation. Carbon, 2004, 42(1): 183–185
14. Fang Z, Tang K B, Lei S J, Li T W. CTAB-assisted hydrothermal synthesis of Ag/C nanostructures. Nanotechnology, 2006, 17(12): 3008–3011
15. Kim B, Sigmund W M. Functionalized multiwall carbon nanotube/gold nanoparticle composites. Langmuir, 2004, 20(19): 8239–8242
16. Biswas S, Kar S, Chaudhuri S. Optical and magnetic properties of manganese-incorporated zinc sulfide nanorods synthesized by a solvothermal process. Journal of Physical Chemistry B, 2005, 109 (37): 17526–17530